Article

A Novel Donor-Acceptor Thiophene-Containing Oligomer Comprising Dibenzothiophene-*S,S*-dioxide Units for Solution-Processable Organic Field Effect Transistor

Xia Luo [1], Zongfan Duan [1,*] , Kang Li [1], Gang He [1], Zhenzhen Liu [1], Hong Luo [1], Jingyu Zhang [2], Jiani Liang [1], Qian Guo [1], Jing Liu [1] and Kai Ding [1]

[1] School of Materials Science and Engineering, Xi'an University of Technology, Xi'an 710048, China; luoxia1223@163.com (X.L.); 18710493483@163.com (K.L.); version521@live.com (G.H.); ycfszd2327@163.com (Z.L.); 15198381707@139.com (H.L.); ginny1997@163.com (J.L.); gq1213440601@163.com (Q.G.); liujyu2022@163.com (J.L.); kai13468697372@sina.com (K.D.)
[2] Materials Corrosion and Protection Key Laboratory of Sichuan Province, Zigong 643000, China; zjy312@suse.edu.cn
* Correspondence: duanzf@xaut.edu.cn; Tel.: +86-29-82312172

Abstract: A π-conjugated thiophene-containing oligomer with a D-A-D-A-D (D: donor, A: acceptor) architecture, namely, 2,6-bis{[*4-(7-n-hexylthiophen-2-yl)thiophen-2-yl*]-(dibenzothiophene-5,5-dioxide-3,3′-diyl)}-bis((2-ethyl-hexyl)oxy)benzo[*1,2-b:4,5-b′*]dithiophen (BDT(DBTOTTH)$_2$), was synthesized by Stille coupling reactions. There are obvious shifts in the Ultraviolet-visible (UV-vis) and photoluminescence (PL) spectra of the thin film relative to its solution, indicating the existence of the π-π stacking in the solid state of the oligomer BDT(DBTOTTH)$_2$. The optical band gap of the oligomer determined from its absorption onset in UV-Vis spectra is 2.25 eV. It agrees with the value of 2.29 eV determined from the cyclic voltammetry (CV) measurement. Its highest occupied and lowest unoccupied molecular orbital (HOMO/LUMO) energy levels, which were calculated from its onset of oxidation and reduction waves in CV curve, are −5.51 and −3.22 eV, respectively. The oligomer is a P-type semiconductor material with a good thermal stability and solubility, which can be used to fabricate organic field effect transistors (OFETs) by the spin coating technique. The OFET with *n*-octadecanylltrichlorosilane (OTS)-modified SiO$_2$ dielectric layer exhibited a mobility of 1.6×10^{-3} cm^2/Vs.

Keywords: thiophene; oligomer; synthesis; semiconductor material; organic field effect transistor

1. Introduction

Over the past decade, π-conjugated polymers and oligomers have been extensively investigated because of their unique photo-electronic properties and potential applications in different organic electronic devices, such as organic light emitting diodes (OLEDs), solar cells and organic field effect transistors (OFETs) [1–3]. The previous work on the design of p-type organic semiconductor molecules suggests that the incorporation of an electron-accepting unit into the molecular backbone of a π-conjugated polymer/oligomer with electron-donating property can result in a small lowering of its highest occupied molecular orbital (HOMO) level, and improve its stability against oxidation. More significantly, it has been confirmed that the formation of donor-acceptor (D-A) structure is beneficial to promote the charge transfer between the donor unit and the acceptor unit in molecules, and obtain a good charge mobility [4]. Therefore, many electron-accepting units including benzothiadiazole [5,6], thiadiazolopyridine [7], naphthalene bisimide [8], thieno-thiadiazole [9], diketopyrrolopyrrole [10–12], bithiophenesulfonamide [13] dithiazole [14], etc., have been introduced into the frameworks of π-conjugated polymers/oligomers. The obtained compounds are used as the excellent organic semiconductor materials in a variety of electronic devices. Among various organic semiconductor materials, π-conjugated

thiophene-containing oligomers have been extensively explored as an active organic semi-conductor material due to their easiness in preparation, purification, chemical structural modification, and moderation of energy levels and optical/electronic properties [15–18]. In this case, it is an interesting subject research on design, synthesis and properties of thiophene-containing oligomers with D-A structure.

Thiophene-*S,S*-dioxides have been examined as an electron-accepting unit. The oligomers containing thiophene-*S,S*-dioxide moieties have the smaller energy gaps, the higher electron affinities and the greater stability than their precursor oligothiophenes [19–21]. The oxidation of the sulfur atom of dibenzothiophene with coplanar rings can yield dibenzothiophene-*S,S*-dioxide (DBTSO), which is a novel electron-accepting unite. Recently, the DBTSO acceptor unit as a central core has been incorporated into the backbone of electron donor oligomers such as fluorene [22–25], carbazole [26], arylamine [27], quinoxaline or pyrazine [28] via co-oligomerization to afford highly efficient OLED materials. Furthermore, our group previously synthesized a D-A-D type oligomer with a DBTSO core and two end-caped phenylthiophene substitutes. Although the optical energy band gap of this oligomer is relative wide (2.52 eV), its bulk-heterojunction (BHJ) solar cell can provide a relative high power conversion efficiency of 0.84% [29,30]. Overall, DBTSO is an ideal electron-accepting unite, and can be used to design and build some potential semiconductor materials with a D-A structure. However, to our knowledge, little attention has been paid to the design and synthesis of thiophene-containing oligomers with more than two DBTSO electron-accepting unites. In addition, there are also no reports on their application in OFET devices.

In this work, a novel π-conjugated thiophene-containing oligomer with two DBTSO electron-accepting unites and a D-A-D-A-D architecture (Figure 1) has been synthesized. It is 2,6-bis{[4-(7-n-hexylthiophen-2-yl)thiophen-2-yl]-(dibenzothiophene-5,5-dioxide-3,3′-diyl)}-bis((2-ethyl-hexyl)oxy)benzo[*1,2-b:4,5-b′*]dithiophen (BDT(DBTOTTH)$_2$), which has a benzo[*1,2-b:4,5-b′*]dithiophene donor core, two DBTSO acceptor intermediaries and two end-capped hexyl dithienyl donor units. Its photophysical properties, energy band gap, molecular orbital energy levels and thermal stability were then characterized using Ultraviolet-visible (UV-vis), photoluminescence (PL) spectra, cyclic voltammetry (CV) and thermogravimetric analysis (TGA). Considering that the oligomer has a large linear π-conjugated and D-A-D-A-D structure, and a good solubility deriving from of hexyl and 2-ethyl-hexyloxy groups, it would be a solution-processable semiconductor material. Therefore, the oligomer BDT(DBTOTTH)$_2$ was further used to fabricate an OFET device by a simple spin coating technique, and a mobility of 1.6×10^{-3} cm^2/Vs was obtained.
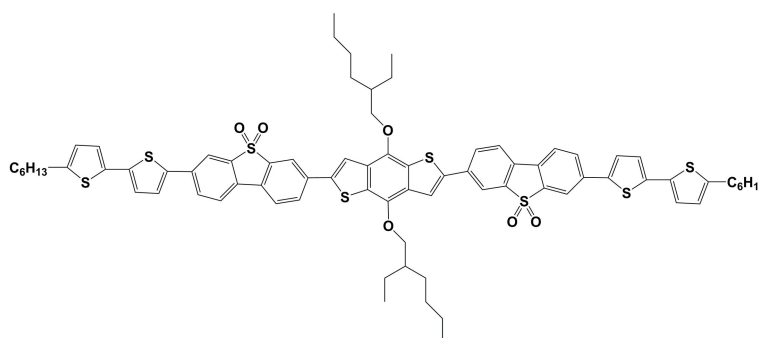

Figure 1. Molecular structure of oligomer BDT(DBTOTTH)$_2$.

2. Experimental

2.1. Materials and Characterization

All chemicals were purchased from Sigma-Aldrich without any further purification. Tetrahydrofuran (THF) and toluene were freshly distilled from sodium and benzophenone, *N,N*,-dimethylformamide (DMF) and dichloromethane were distilled from CaH$_2$ under N$_2$ atmosphere prior to use. Thin-layer chromatography (TLC) was performed using pre-coated silica gel plates (Merck Kieselgel 60F$_{254}$) and column chromatography

was employed using silica gel (Merk, 130–270 mesh). Nuclear magnetic resonance (NMR) spectra for ^{1}H and ^{13}C spectra were recorded on spectrometer ((INOVA-400MHz)) using deuterated chloroform ($CDCl_3$) as a solvent. Additionally, mass spectra were acquired on a matrix-assisted laser desorption/ionization-time-of-flight (Bruker ultraflextreme MALDI-TOF) mass spectrometer. All chemical shifts were shown in parts per million (ppm) with tetramethylsilane as an internal standard. The UV-vis spectra of the oligomer in a chloroform solution (10^{-6} M) and a thin film were recorded on a U-3900H spectrophotometer. The thickness of the film is about 50 nm, which drop-casted from the tetrachlorethan solution on a quartz substrate. The PL spectra of the oligomer in the solution and thin film were then measured with a FLUOROMAX-4 fluorospectrophotometer ($\lambda_{excitation}$ = 318 nm). The CV measurement of the oligomer was performed on PARSTAT-4000A using a three-electrode cell at room temperature. In CV measurement, the oligomer was dissolved in an anhydrous dichloromethane in a concentration of 10^{-3} M, containing 0.1 M of tetrabutylammonium hexafluorophosphate (Bu_4NPF_6) as the supporting electrolyte. The working electrode and counter electrode was a platinum stick and platinum wire, respectively. In addition, a calomel electrode was used as the reference electrode, which had been calibrated against ferrocene/ferrocenium. The TGA was performed using a SHIMADZU, DTG-60H instrument at a heating rate of 10 °C/s in nitrogen atmosphere. Transistor measurements were performed in air using an Aglient 4155C semiconductor parameter analyzer.

2.2. Oligomer Synthesis

Figure 2 outlines the synthetic pathway of the oligomer $BDT(DBTOTTH)_2$. 2-Hexylthiophene (**1**), 2-(trimethylstannyl)-5-hexylthiophene (**2**) and 5-hexyl-2,2'-bithiophen (3) were prepared according to literature procedures [31]. The compound (**3**) reacted with *n*-butyllithium and trimethyltin chloride to produce 5-(trimethylstannyl)-5'-hexyl-2,2'-bithiophene (**4**) [32]. Because the stannyl compound (**4**) is liable to acids, it was used without any further purification. 3,7-Dibromodibenzothiophene-*S,S*-dioxide (**7**) was obtained by two steps: the oxidation of dibenzothiophene ((**5**)→(**6**)) and bromination with bromine/acetic acid((**6**)→(**7**)) [33]. The intermediate, 3-bromo-7-(5'-hexyl-2,2'-bithiophen-5-yl)dibenzo[*b,d*]thiophene *S,S*-dioxide (**8**), was prepared by the Stille cross-coupling reaction of 5-trimethylstannyl-5'-hexyl-2,2'-bithiophene (**4**) with 3,7-dibromodibenzothiophene-*S,S*-dioxide (**7**) in the presence of $Pd(PPh_3)_4$ catalyst. The 3-thiophene carbonyl chloride (**10**) was obtained from the reaction of commercially 3-thiophenecarboxylic acid (**9**) with thionyl chloride. The amidation reaction of 3-thiophene carbonyl chloride (**10**) with diethylamide gave the corresponding *N,N*-diethylthiophene-3-carboxamide (**11**). Benzo[*2,3-b:5,6-b'*]dithiophene-4,8-dione (**12**) was prepared by the reaction of *N,N*-diethylthiophene-3-carboxamide (**11**) with *n*-butyllithium at −78 °C under nitrogen atmosphere. The soluble 4,8-bis(octyloxy)benzo[*1,2-b:4,5-b'*]dithiophene (**13**) was obtained in moderate yield from benzo[*2,3-b:5,6-b'*] dithiophen e-4,8-dione (**12**) by being treated with a mixture of Zn powder, NaOH and deionized water, and finally reacted with 2-ethylhexyl bromide in the presence of (*n*-Bu)$_4$NBr catalyst [34]. The compound 2,6-bis(trimethylstannane)-4,8-bis((2-ethylhexyl)oxy)benzo[*1,2-b:4,5-b'*]dithiophene (**14**) was prepared using a similar methodology to stannane (**2**) [35]. The synthesis of the oligomer $BDT(DBTOTTH)_2$ was also commenced using the Stille cross-coupling catalyzed by $Pd(PPh_3)_4$. To ensure completion of the coupling reaction, an excess of the bromide (**8**) was used [36].
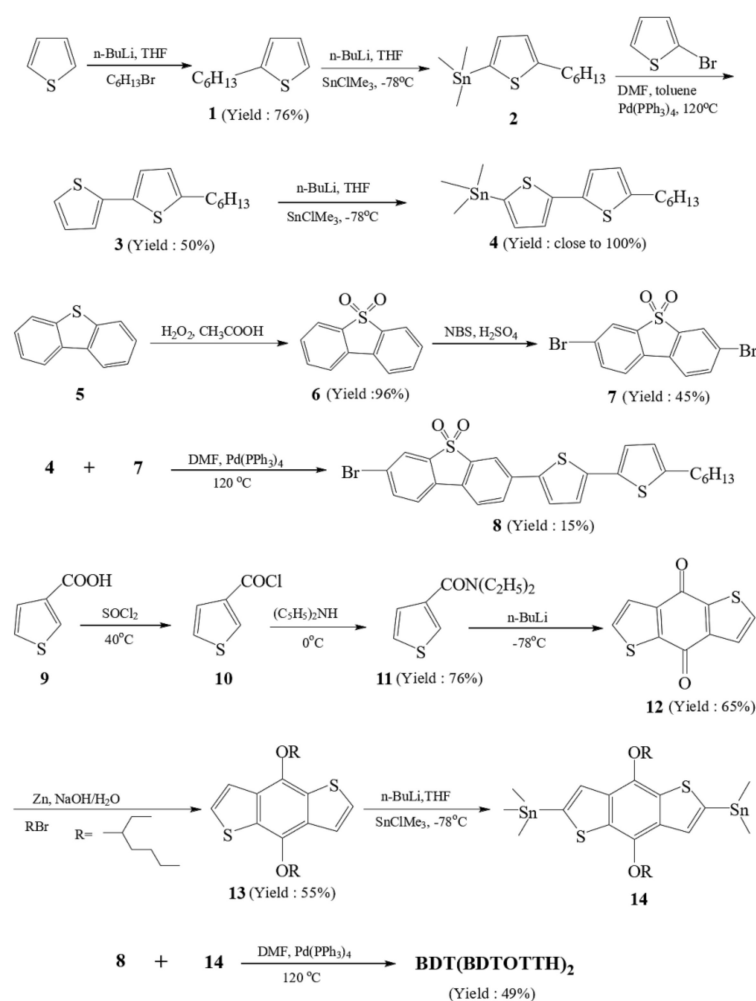
Figure 2. Synthetic pathway for the oligomer BDT(DBTOTTH)$_2$.

2.2.1. Synthesis of
3-bromo-7-(5′-hexyl-2,2′-bithiophen-5-yl)dibenzo[b,d]thiophene-*S*,*S*-dioxide (**8**)

5-Trimethylstannyl-5′-hexyl-2,2′-bithiophene (2.19 g, 5.33 mmol), 3,7-dibromodibenzot
hiophene-*S*,*S*-dioxide (5.98 g, 16 mmol), Pd(PPh$_3$)$_4$ (46 mg, 0.04 mmol) and anhydrous
N,*N*-dimethylformamide (DMF, 50 mL) were successively added into a 100 mL three-neck
round-bottomed flask. After deoxygenating with dry nitrogen for 30 min, the mixture was
stirred at 120 °C for 30 h under nitrogen atmosphere. The reactants were cooled to room
temperature and the resulting yellow solid was then collected by filtration. The filtrate was
extracted with dichloromethane (100 mL) for 3 times. The organic layer was dried over
MgSO$_4$, filtered and evaporated. Two parts of solid were combined and then purified by
column chromatography using petroleum ether/dichloromethane (3:1) as eluent (Rf = 0.52).
A yellow solid of 0.43 g was obtained with a yield of 15%. ^{1}H NMR (CDCl$_3$, 400 Hz,
δ/ppm): 8.28 (s, 1H), 8.15 (s, 1H), 8.03 (d, *J* = 6.0 Hz, 1H), 7.94 (d, *J* = 6.4 Hz, 1H), 7.79 (d,
J = 6.4 Hz, 1H), 7.74 (d, *J* = 6.4 Hz, 1H), 7.65 (d, *J* = 7.6 Hz, 1H), 7.62 (d, *J* = 7.6 Hz, 1H),
7.51 (d, *J* = 7.6 Hz, 1H), 7.46 (d, *J* = 7.6 Hz, 1H), 2.50 (t, *J* = 8.4 Hz, 2H), 1.58–1.81 (m, 2H),
1.17–1.45(m, 6H), 0.72–0.94 (m, 3H). ^{13}C NMR (CDCl$_3$, 100 MHz, ppm): δ 145.21, 144.28,
142.90, 140.87, 139.25, 132.45, 129.85, 124.03, 123.48, 122.32, 120.35, 117.91, 115.88, 114.03,
40.68, 31.90, 29.67, 22.67, 14.09. MALDI-TOF MS (*m*/*z*): calcd for C$_{26}$H$_{23}$BrO$_2$S$_3$, 542.0044,
found; 542.0042. Melting point: 370–372 °C.

2.2.2. Synthesis of the Oligomer BDT(DBTOTTH)$_2$

2,6-Bis(trimethylstannane)-4,8-bis((2-ethylhexyl)oxy)benzo[*1,2-b:4,5-b′*]dithiophene (0.43 g,
0.56 mmol), 3-bromo-7-(5′-hexyl-2,2′-bithiophen-5-yl)dibenzo[*b*,*d*]thiophene-*S*,*S*-dioxide

(0.82 g, 1.5 mmol), anhydrous DMF (50 mL) and Pd(PPh$_3$)$_4$ (17 mg, 0.015 mmol) were added to a 100 mL three-neck round-bottomed flask in turn. The mixture was deoxygenated with nitrogen for 30 min, and then stirred at 120 °C for 30 h under nitrogen. The resulting solid was collected by filtration, and washed with KF solution (100 mL, 8%), water (100 mL) and dichloromethane (50 mL) in turn. The obtained crude product was then purified by column chromatography using petroleum ether/dichloromethane (1:1) as an eluent for 3 times (Rf = 0.43). A yellowish-brown solid of 0.38 g was obtained with a yield of 49%. The melting point (m.p.) is higher than 270 °C. ^{1}H NMR (CDCl$_3$, 400 Hz, δ/ppm): 8.33 (s, 4H), 7.87 (d, J = 5.6 Hz, 4H), 7.80 (d, J =6.4 Hz, 4H), 7.70 (s, 2H), 7.63 (d, J =7.2 Hz, 2H), 7.58 (d, J = 7.2 Hz, 2H), 7.48 (d, J =7.2 Hz, 2H), 7.42 (d, J = 7.2 Hz, 2H), 4.17–4.22(m, 2H), 4.05–4.14 (m, 2H), 2.43 (t, J = 8.4 Hz, 4H), 1.84–2.15 (m, 2H), 1.54~1.64 (m, 8H), 1.04~1.37 (m, 24H), 0.64~0.89 (m, 18H). ^{13}C NMR (CDCl$_3$, 100 MHz, ppm): δ 144.41, 143.25, 142.51, 137.33, 135.03, 135.00, 134.32, 132.72, 131.12, 129.05, 128.84, 126.89, 125.78, 124.88, 123.11, 122.85, 119.71, 119.04, 72.01, 39.30, 38.99, 32.14, 31.74, 30.79, 29.91, 27.94, 22.93, 19.40, 14.09. MALDI-TOF MS (m/z): calcd for C$_{78}$H$_{82}$O$_6$S$_8$, 1370.3877; found, 1370.3874.

2.2.3. Fabrication of OFET Device

The cost of device fabrication is a vital factor for the application of organic electron devices. The spin-coating has been proven to be an easier and low cost fabrication process compared with the vacuum evaporation. In this work, the oligomer BDT(DBTOTTH)$_2$ was used to fabricate OFET devices by the spin coating method. As shown in Figure 3, the OTFT device has "top contact" configuration. The *n*-doped silicon substrate functions as the gate electrode, and a thermally grown 300 nm silicon dioxide (SiO$_2$) modified by an *n*-octadecanylltrichlorosilane self-assembled monolayer layer (OTS-SiO$_2$) works as the insulating dielectric layer. The OTS-SiO$_2$/Si was prepared by SiO$_2$/Si being treated with a toluene solution of OTS (10 mg/mL) at 60 °C for 20 min. Its capacitance per unit area is 11.0 nF/cm^2. The thin film of BDT(DBTOTTH)$_2$ was fabricated on OTS-SiO$_2$/Si substrate by spin coating in a tetrachlorethan solution (2 mg/mL) at 1500 rpm for 100 s and then annealed at 150 °C for 30 min. As a result, a BDT(DBTOTTH)$_2$ semiconductor active layer with a thickness of about 80 nm was obtained. The source (S) and drain (D) Au electrodes were deposited onto BDT(DBTOTTH)$_2$ layer through a shadow mask by vacuum thermal deposition method. The thickness of Au electrode is about 100 nm, and the channel length and width of the OTFT device are 50 and 500 μm, respectively.
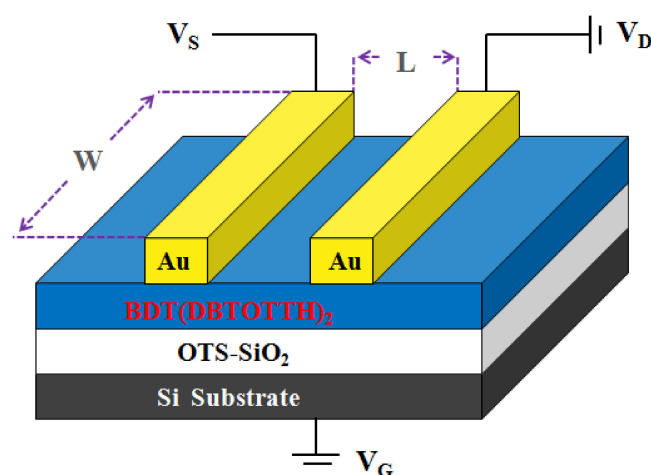

Figure 3. Schematic configuration of the top contact OFET device based on BDT(DBTOTTH)$_2$.

2.3. Results and Discussion

2.3.1. Synthetic Methodology

For the synthesis of thiophene-containing oligomers, one of the most useful procedures in the formation of C-C σ-bonds is the metal-promoted coupling reaction of organic halides.

In this work, the palladium(0)-catalyzed Stille cross-coupling reaction was used as a main reaction type to prepare the oligomer BDT(DBTOTTH)$_2$ due to its tolerance to a variety of functional groups (e.g., CO$_2$R, CHO, OH, SO$_2$). In order to obtain a single coupling product (**8**) as much as possible, an excess of the bromide (**7**) was used. The optimum mole ratio of stannyl compound (**5**) and bromide (**7**) was 1:3. The compound (**8**) and the target oligomer BDT(DBTOTTH)$_2$ were soluble in common solvents such as dichloromethane, chloroform, THF and tetrachlorethan. They were purified by column chromatography, owing to the contribution from *n*-hexyl or/and 2-ethyl-hexyloxy groups.

2.3.2. Photophysical Properties

As shown in Figure 4, the oligomer in dilute CH$_2$Cl$_2$ solution has the absorption maximum value at 359 nm and a broad shoulder peak at 425 nm, whereas in the thin film, the absorption band of the oligomer becomes relatively broader and less structured. The maximum absorption peak displays a blue-shift about 7 nm relative to that of its corresponding solution. The blue-shift should attribute to the formation of the H-aggregate in the solid state [37], which is usually observed in excellent semiconductor materials. In H-aggregates, since the molecules are closely π-stacked in a face-to-face alignment, the neighboring molecules also interact in the ground state [38]. The absorption onset (λ_{edge}) of the oligomer film in UV-Vis spectra is 550 nm. According to Equation (1),

$$E_g^{opt}(\text{eV}) = 1240/\lambda_{edge}(\text{nm}) \tag{1}$$

the optical band gap of the oligomer was calculated to be 2.25 eV. This band gap is moderate, and very close to that of pentacene (2.2 eV), which is the most well-known OFET material [39]. The pronounced changes in the absorption spectra are a result of the delocalization of the exciton within co-facial stacks induced by the π-π interactions, which is also evidenced by a related red-shift of the PL spectra (Figure 5). The emission spectrum of the oligomer BDT(DBTOTTH)$_2$ shows strong blue-green fluorescence in the diluted solution, and exhibits a maximum emission peak at 464 nm with a broad shoulder peak ranging from 540 to 610 nm. The emission spectrum of the oligomer BDT(DBTOTTH)$_2$ in the thin film has a similar pattern as that in solution except for an obvious red shift. The maximum emission peak of the oligomer in the film is located at 578 nm. Compared with that in the solution, the emission spectrum is bathochromically shifted by 114 nm.
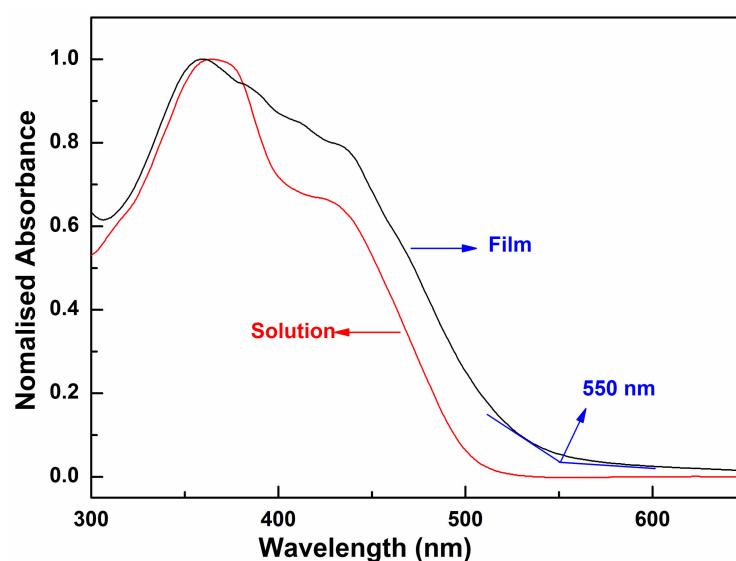

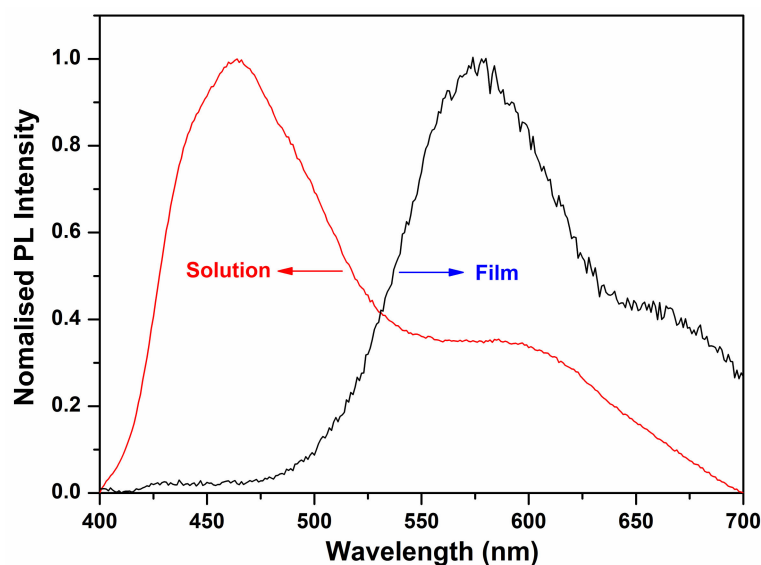**Figure 4.** UV-vis absorption spectra of oligomer BDT(DBTOTTH)$_2$.

Figure 5. PL spectra of the oligomer BDT(DBTOTTH)$_2$.

2.3.3. Electrochemical Properties

To understand the charge transport properties, and to determine the HOMO and lowest unoccupied molecular orbital (LUMO) levels of the oligomer, the redox properties of the oligomer BDT(DBTOTTH)$_2$ were investigated by cyclic voltammetry (CV). As shown in Figure 6, the oligomer shows an irreversible oxidation wave, and has an onset oxidation potential of 1.11 eV. It is well known that the HOMO levels of organic compounds can be calculated according to their onset oxidation potentials and the empirical Equation (2).

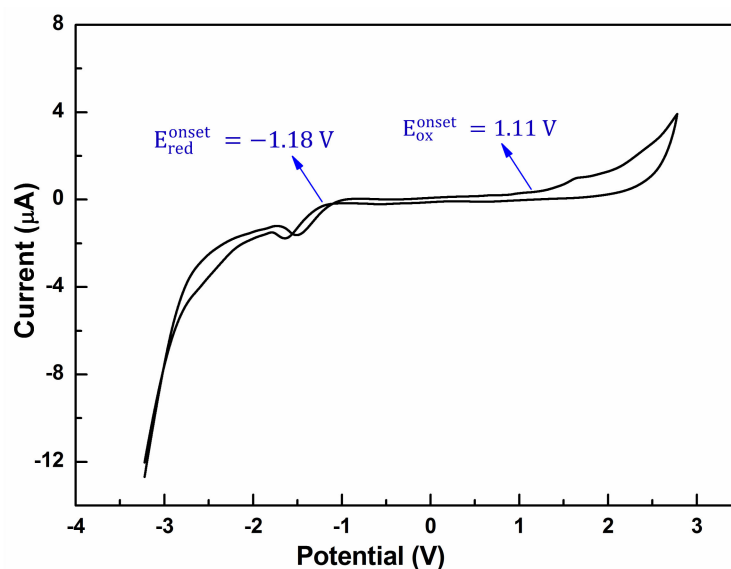$$\text{E}_{\text{HOMO}} = -e\left(E_{ox}^{onset} + 4.4\right) \text{ (eV)} \qquad (2)$$

Figure 6. Cyclic voltammogram curve of the oligomer BDT(DBTOTTH)$_2$.

Based on Equation (2), the HOMO level of the oligomer BDT(DBTOTTH)$_2$ was calculated to be −5.51 eV. The stability of organic semiconducting materials toward oxidative doping is related to their HOMO energy levels. The environmental stability can be improved by lowering the HOMO energy level to minimize the possibility of p-doping by ambient oxygen. Compared with that of pentacene (−4.56 eV) [40], rubrene (−4.69 eV) [41] and sixthiophene (−4.99 eV) [40], the HOMO energy level of the oligomer BDT(DBTOTTH)$_2$

is relatively lower. This indicates that the oligomer is oxidatively stable in air. It is a key requirement for organic devices. Furthermore, the HOMO energy level is close to the work function of gold (-5.1 eV) [42]. It suggests that the gold would be the best optimum selection for source and drain electrodes in OFET devices based on the oligomer BDT(DBTOTTH)$_2$. The CV curve also includes a reduction wave, an onset reduction potential is at -1.18 V. According to the empirical Equation (3), the determined LUMO energy level of the oligomer is -3.22 eV.

$$\mathrm{E_{LUMO}} = -e\left(E_{red}^{onset} + 4.4\right) \text{ (eV)} \tag{3}$$

2.3.4. Thermal Analysis

The thermal stability of the oligomer BDT(DBTOTTH)$_2$ was evaluated by TGA in N$_2$ atmosphere. As shown in Figure 7, the oligomer exhibited good thermal stability and the losing less than 5% of weight was observed higher than 400 °C. It indicates that the oligomer BDT(DBTOTTH)$_2$ exhibits good thermal stability.
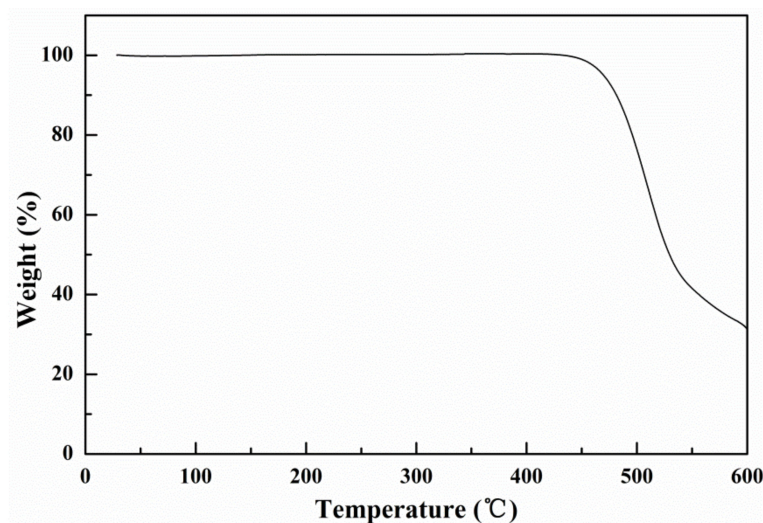

Figure 7. TGA curve of the oligomer BDT(DBTOTTH)$_2$.

2.3.5. OFET Performance

Figure 8a shows the relationships between the drain-current (I$_D$) and drain-source voltage (V$_{DS}$) at different gate-source voltages (V$_{GS}$) from -40 to -70 V for the OFET device using OTS/SiO$_2$ as the insulating dielectric layer. The function of the transistor with the negative gate voltage range suggests that BDT(DBTOTTH)$_2$ is a p-type semiconductor material. The output characteristics show a good saturation behavior and clear saturation currents that are quadratic to the gate bias. Furthermore, as a more negative V$_{GS}$ was used, more holes were induced in the accumulation layer of the organic semiconductor. As a result, an increased I$_{DS}$ was achieved. The most critical properties of an OFET device are the charge mobility (μ_{sat}) and I$_{on}$/I$_{off}$ current ratio. The charge mobility is the average drift velocity per unit electric field, and it can be calculated in the saturation regime using following Equation (4),

$$\mu_{sat}(V_{GS}) = \frac{2L}{WC_i}\left[\frac{\partial\sqrt{I_D(V_{GS})}}{\partial V_{GS}}\right]^2 \quad (|V_{DS}| \geq |V_{GS} - V_{TH}|) \tag{4}$$

where μ_{sat} is the field-effect mobility, W the channel width (500 μm), L the channel length (50 μm), C_i the capacitance of the insulator layer, I$_D$ the drain-current, V_{GS}, V_{DS} and V_{TH} are the gate voltage, drain-source voltage and threshold voltage. In order to calculate the field-effect mobility, V_{TH} were determined firstly. Figure 8b shows the relationship between the square root of I$_D$ and V$_{GS}$ at $V_{DS} = -50$ V. From the slope of the plot of $(I_D)^{1/2}$ versus V_{GS}.

The V_{TH} of the OFET device was determined to be -44 V. Using Equation (4), the calculated mobility value of the OFET device was 1.6×10^{-3} cm^2/Vs. Its I_{on}/I_{off} current ratio, which was defined as the ratio of current flow between the source and drain when there was no gate bias and the current flow at maximum gate bias, was higher than 1.0×10^4. The mobility value of the OFET device is really not high. It is well known that the performance of OFET devices depends not on the molecule structure of semiconductor materials, but also on other experimental factors such as purity, dielectric layer, thickness and morphology of semiconductor layer, and electrode and structure of the device. Although the mobility of the OFET device based on the oligomer BDT(DBTOTTH)$_2$ is lower than those of many reported thiophe-containing oligomers, the further improvements of its OFET performance can be expected in our future study.
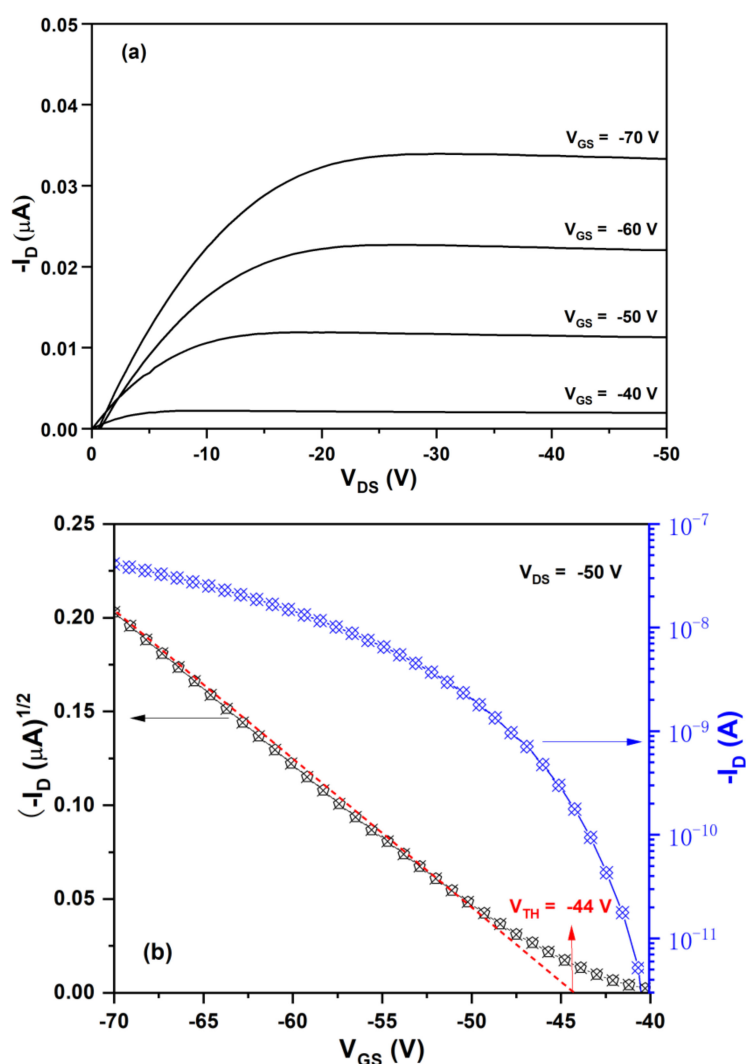

Figure 8. (**a**) Output characteristics and (**b**) transfer characteristics of the OFET device based on BDT(DBTOTTH)$_2$.

3. Conclusions

A novel π-conjugated D-A-D-A-D type thiophene-containing oligomer BDT(DBTOTTH)$_2$ comprising a benzo[*1,2-b:4,5-b'*]dithiophene donor core, two DBTSO acceptor intermediaries and two end-capped hexyl dithienyl donor units were designed and synthesized. The oligomer exhibits the energy band gap of 2.25 eV, the HOMO level of -5.51 eV, and LUMO level -3.22 eV. The remarkable shifts in UV-vis and PL spectra for the thin film relative to its corresponding solution indicate the existence of intermolecular π-π stacking in the solid state. The oligomer has good solubility owning to the contribution of hexyl and

2-ethyl-hexyloxy groups, and it can be used to fabricate OFET devices by the spin coating method. The oligomer is p-type semiconductor material, and its OFET device shows the mobility of 1.6×10^{-3} cm^2/Vs.

Author Contributions: Methodology, X.L. and Z.D.; validation, K.L., G.H. and Z.L.; data curation, H.L., J.L. (Jiani Liang), Q.G., J.L. (Jing Liu) and K.D.; writing—original draft preparation, X.L.; writing—review and editing, X.L. and Z.D.; supervision and funding acquisition, J.Z. All authors have read and agreed to the published version of the manuscript.

Institutional Review Board Statement: Not applicable.

Informed Consent Statement: Not applicable.

Data Availability Statement: Not applicable.

Conflicts of Interest: The authors declare no conflict of interest.

Sample Availability: Samples of the compounds are not available from the authors.

References

1. Fu, Y.; Qu, J.; Geng, Y.; Wang, B.; Han, Y.; Xie, Z. Insight into correlation between molecular length and exciton dissociation, charge transport and recombination in Polymer: Oligomer based solar cells. *Org. Electron.* **2018**, *58*, 75–81. [CrossRef]
2. Bala, I.; Yang, W.Y.; Gupta, S.P.; De, J.; Yadav, R.A.K.; Singh, D.P.; Dubey, D.K.; Jou, J.H.; Douali, R.; Pal, S.K. Room temperature discotic liquid crystalline triphenylene-pentaalkynylbenzene dyads as an emitter in blue OLEDs and their charge transfer complexes with ambipolar charge transport behavior. *J. Mater. Chem. C* **2019**, *7*, 5724–5738. [CrossRef]
3. Pachariyangkun, A.; Suda, M.; Hadsadee, S.; Jungsuttiwong, S.; Nalaoh, P.; Pattanasattayavong, P.; Sudyoadsuk, T.; Yamamoto, H.M.; Promarak, V. Effect of thiophene/furan substitution on organic field effect transistor properties of arylthiadiazole based organic semiconductors. *J. Mater. Chem. C* **2020**, *8*, 17297–17306. [CrossRef]
4. Feng, L.Z.; Shi, X.F.; Xie, J.; Zheng, D.M.; Niu, H.H.; Huang, Y.B.; Ye, L.Y.; Yin, Y.W.; Tu, S. Synthesis, characterization, and electroluminescent properties of monodisperse oligofluorenes as emissive materials for organic electroluminescent devices. *J. Taiwan Inst. Chem. Eng.* **2017**, *71*, 69–76. [CrossRef]
5. Skorotetcky, M.S.; Krivtsova, E.D.; Borshchev, O.V.; Surin, N.M.; Svidchenko, E.A.; Fedorov, Y.V.; Pisarev, S.A.; Ponomarenko, S.A. Influence of the structure of electron-donating aromatic units in organosilicon luminophores based on 2,1,3-benzothiadiazole electron-withdrawing core on their absorption-luminescent properties. *Dye. Pigment.* **2018**, *155*, 284–291. [CrossRef]
6. Zhang, S.; Bauer, N.E.; Kanal, I.Y.; You, W.; Hutchison, G.R.; Meyer, T.Y. Sequence effects in donor-acceptor oligomeric semiconductors comprising benzothiadiazole and phenylenevinylene monomers. *Macromolecules* **2017**, *50*, 151–161. [CrossRef]
7. Ishi-i, T.; Tanaka, H.; Koga, H.; Tanaka, Y.; Matsumoto, T. Near-infrared fluorescent organic porous crystal that responds to solvent vapors. *J. Mater. Chem. C* **2020**, *8*, 12437–12444. [CrossRef]
8. Rybakiewicz, R.; Glowacki, E.D.; Skorka, L.; Pluczyk, S.; Zassowski, P.; Apaydin, D.H.; Lapkowski, M.; Zagorska, M.; Pron, A. Low and high molecular mass dithienopyrrole–naphthalene bisimide donor–acceptor compounds: Synthesis, electrochemical and spectroelectrochemical behavior. *Chem. A Eur. J.* **2017**, *23*, 2839–2851. [CrossRef]
9. Cimrová, V.; Výprachtický, D.; Pokorná, V. Donor-acceptor copolymers containing bithiophene and dithiophenylthienothiadiazole units with fast electrochromic response. *J. Mater. Chem. C* **2019**, *7*, 8575–8584. [CrossRef]
10. Truong, N.T.T.; Nguyen, L.T.; Mai, H.L.T.; Doan, B.K.; Tran, D.H.; Truong, K.T.; Nguyen, V.Q.; Nguyen, L.T.T.; Hoang, M.H.; van Pham, T.; et al. Phenothiazine derivatives, diketopyrrolopyrrole-based conjugated polymers: Synthesis, optical and organic field effect transistor properties. *J. Polym. Res.* **2020**, *27*, 1–13. [CrossRef]
11. Lo, C.K.; Wang, C.Y.; Oosterhout, S.D.; Zheng, Z.; Yi, X.; Fuentes-Hernandez, C.; So, F.; Coropceanu, V.; Brédas, J.L.; Toney, M.F.; et al. Langmuir-Blodgett Thin Films of Diketopyrrolopyrrole-Based Amphiphiles. *ACS Appl. Mater. Interfaces.* **2018**, *10*, 11995–12004. [CrossRef] [PubMed]
12. Lim, B.; Han, S.Y.; Jung, S.H.; Jung, Y.J.; Park, J.M.; Lee, W.; Shim, H.S.; Nah, Y.C. Synthesis and electrochromic properties of a carbazole and diketopyrrolopyrrole-based small molecule semiconductor. *J. Ind. Eng. Chem.* **2019**, *80*, 93–97. [CrossRef]
13. Melkonyan, F.S.; Zhao, W.; Drees, M.; Eastham, N.D.; Leonardi, M.J.; Butler, M.R.; Chen, Z.; Yu, X.; Chang, R.P.H.; Ratner, M.A.; et al. Bithiophenesulfonamide (BTSA) Building Block for π-Conjugated Donor-Acceptor Semiconductors. *J. Am. Chem. Soc.* **2016**, *138*, 6944–6947. [CrossRef] [PubMed]
14. Ma, S.; Zhang, G.; Wang, F.; Dai, Y.; Lu, H.; Qiu, L.; Ding, Y.; Cho, K. Tuning the Energy Levels of Aza-Heterocycle-Based Polymers for Long-Term n-Channel Bottom-Gate/Top-Contact Polymer Transistors. *Macromolecules* **2018**, *51*, 5704–5712. [CrossRef]

15. Turkoglu, G.; Cinar, M.E.; Ozturk, T. Thiophene-Based Organic Semiconductors. *Top. Curr. Chem.* **2017**, *375*, 79–123. [CrossRef] [PubMed]
16. Oyama, T.; Mori, T.; Hashimoto, T.; Kamiya, M.; Ichikawa, T.; Komiyama, H.; Yang, Y.S.; Yasuda, T. High-Mobility Regioisomeric Thieno[f,f']bis[1]benzothiophenes: Remarkable Effect of Syn/Anti Thiophene Configuration on Optoelectronic Properties, Self-Organization, and Charge-Transport Functions in Organic Transistors. *Adv. Electron. Mater.* **2017**, *4*, 1700390. [CrossRef]
17. Milad, R.; Essalah, K.; Abderrabba, M. Optoelectronic and conductivity of Л-conjugated polymers based on phenylenevinylene, 1,3,4-thiadiazole and thiophene: Suitable candidates for n-type organic semiconductors. *J. Phys. Org. Chem.* **2018**, *31*, e3750. [CrossRef]
18. Yevlampieva, N.P.; Khurchak, A.P.; Luponosov, Y.N.; Kleimyuk, E.A.; Ponomarenko, S.A.; Ryumtsev, E.I. Optical and electro-optical properties of silicon-contaning thiophene derivatives of star-shaped and dendritic structure. *Russ. J. Appl. Chem.* **2013**, *86*, 747–755. [CrossRef]
19. Dell, E.J.; Campos, L.M. The preparation of thiophene-S,S-dioxides and their role in organic electronics. *J. Mater. Chem.* **2012**, *22*, 12945–12952. [CrossRef]
20. Meng, B.; Miao, J.; Liu, J.; Wang, L. A new polymer electron acceptor based on thiophene-*S*,*S*-dioxide unit for organicphotovoltaics. *Macromol. Rapid Commun.* **2017**, *1*, 1700505.
21. Hu, Q.; Jiang, H.; Cui, Z.; Chen, W. An insight into the effect of *S*,*S*-dioxided thiophene on the opto-physical/electro-chemical properties and light stability for indophenine derivatives. *Dye. Pigment.* **2020**, *173*, 107891. [CrossRef]
22. Huang, C.; Cheng, C.; Shih, Y. All-solution-processed fluorene/dibenzothiophene-*S*,*S*-dioxide blue co-oligomer light-emitting diodes with an electron transporting PEI/ultrafine-ZnO-nanoparticle bilayer. *RSC Adv.* **2017**, *7*, 41855–41861. [CrossRef]
23. Chulkin, P.; Vybornyi, O.; Lapkowski, M.; Skabara, P.J.; Data, P. Impedance spectroscopy of OLEDs as a tool for estimating mobility and the concentration of charge carriers in transport layers. *J. Mater. Chem. C* **2018**, *6*, 1008–1014. [CrossRef]
24. Zheng, X.; Liu, Y.; Zhu, Y.; Ma, F.; Feng, C.; Yu, Y.; Hu, H. Efficient inkjet-printed blue OLED with boosted charge transport using host doping for application in pixelated display. *Opt. Mater.* **2020**, *101*, 109755. [CrossRef]
25. Song, C.; Hu, Z.; Luo, Y.; Cun, Y.; Wang, L.; Ying, L.; Huang, F. Organic/inorganic hybrid EIL for all-solution-processed OLEDs. *Adv. Electron. Mater.* **2018**, *4*, 1700380. [CrossRef]
26. Colella, M.; Pander, P.; Monkman, A.P. Solution processable small molecule based TADF exciplex OLEDs. *Org. Electron.* **2018**, *62*, 168–173. [CrossRef]
27. Hsu, C.; Hsieh, M.; Tsai, M.; Li, Y.; Huang, C.; Su, Y. Fluorescent oligomers of dibenzothiophene-*S*,*S*-dioxide derivatives: The interplay of crystal conformations and photo-physical properties. *Tetrahedron* **2012**, *68*, 5481–5491. [CrossRef]
28. Huang, T.H.; Whang, W.T.; Shen, J.Y.; Wen, Y.S.; Lin, J.T.; Ke, T.H.; Chen, L.Y.; Wu, C.C. Dibenzothiophene/Oxide and Quinoxaline/Pyrazine Derivatives Serving as Electron-Transport Materials. *Adv. Funct. Mater.* **2006**, *16*, 1449–1456. [CrossRef]
29. Fujii, S.; Duan, Z.; Okukawa, T.; Yanagi, Y.; Yoshida, A.; Tanaka, T.; Zhao, G.; Nishioka, Y.; Kataura, H. Synthesis of novel thiophene-phenylene oligomer derivatives with a dibenzothiophene-5,5-dioxide core for use in organic solar cells. *Phys. Status Solidi B* **2012**, *249*, 2648–2651. [CrossRef]
30. Duan, Z.; Huang, X.; Fujii, S.; Kataura, H.; Nishioka, Y. Novel Phenylene-Thiophene Oligomer Derivatives with Dibenzothiophene 5,5-Dioxide Core: Synthesis, Characterization, and Applications in Organic Solar Cells. *Chem. Lett.* **2012**, *41*, 363–365. [CrossRef]
31. Nicolas, Y.; Blanchard, P.; Levillain, E.; Allain, M.; Mercier, N.; Roncali, J. Planarized star-shaped oligothiophenes with enhanced pi-electron delocalization. *Org. Lett.* **2004**, *6*, 273–276. [CrossRef] [PubMed]
32. Yu, C.Y.; Ko, B.T.; Ting, C.; Chen, C.P. Two-dimensional regioregular polythiophenes with conjugated side chains for use in organic solar cells. *Sol. Energ. Mater. Sol. Cells* **2009**, *93*, 613–620. [CrossRef]
33. Camurlu, P.; Durak, T.; Balan, A.; Toppare, L. Electronic and optical properties of dibenzothiophen-*S*,*S*-dioxide and EDOT based conducting polymers. *Synth. Met.* **2011**, *161*, 1898–1905. [CrossRef]
34. Zhou, X.L.; Li, X.H.; Liu, Y.W.; Li, R.J.; Jiang, K.J.; Xia, J.B. Investigation of benzo(1,2-b:4,5-b')dithiophene as a spacer in organic dyes for high effificient dye-sensitized solar cell. *Org. Electron.* **2015**, *25*, 245–253. [CrossRef]
35. Gao, Z.; Qu, B.; Wu, H.M.; Yang, H.S.; Gao, C.; Zhang, L.P.; Xiao, L.X.; Chen, Z.J.; Wei, W.; Gong, Q.H. A fluorine-functionalized alternating polymer with benzo[*1,2-b:4,5-b'*]dithiophene and quinoxaline segments for photovoltaic devices. *Synth. Met.* **2013**, *172*, 69–75. [CrossRef]
36. Ma, P.; Wang, C.; Wen, S.; Wang, L.; Shen, L.; Guo, W.; Ruan, S. Small molecules based on tetrazine unit for efficient performance solution-processed organic solar cells. *Sol. Energy Mater. Sol. Cells* **2016**, *155*, 30–37. [CrossRef]
37. Holzmueller, F.; Gräßler, N.; Sedighi, M.; Müller, E.; Knupfer, M.; Vandewal, K.; Koerner, C.; Leo, K. H-aggregated small molecular nanowires as near infrared absorbers for organic solar cells. *Org. Electron.* **2017**, *45*, 198–201. [CrossRef]
38. Duan, Z.F.; Hu, D.W.; Ohuchi, H.; Zhao, M.Q.; Zhao, G.Y.; Nishioka, Y. Organic field-effect transistors based on two phenylene-thiophene oligomer derivatives with a biphenyl or fluorene core. *Synth. Met.* **2012**, *162*, 1292–1298. [CrossRef]
39. Owens, F.J. Pentacene and poly-pentacene as graphene nanoribbons. *Solid State Commun.* **2014**, *185*, 58–61. [CrossRef]
40. Takimiya, K.; Kunugi, Y.; Otsubo, T. Development of New Semiconducting Materials for Durable High-performance Air-stable Organic Field-effect Transistors. *Chem. Lett.* **2007**, *36*, 578–583. [CrossRef]
41. Filho, D.A.d.; Kim, E.G.; Brédas, J.L. Transport properties in the rubrene crystal: Electronic coupling and vibrational reorganization energy. *Adv. Mater.* **2005**, *17*, 1072–1076. [CrossRef]

42.	Park, Y.J.; Song, A.R.; Walker, B.; Seo, J.H.; Chung, K.B. Hybrid ZnON–Organic Light Emitting Transistors with Low Threshold Voltage <5 V. *Adv. Opt. Mater.* **2019**, *7*, 1801290.